Journal of Applied Physics ARTICLE pubs.aip.org/aip/jap

Stability transition conditions of dislocation cores and Peierls stress

Cite as: J. Appl. Phys. **137**, 095102 (2025); doi: 10.1063/5.0247955
Submitted: 9 November 2024 · Accepted: 10 February 2025 ·
Published Online: 4 March 2025

Shaofeng Wang[a)]

AFFILIATIONS

Department of Physics and Institute for Structure and Function, Chongqing University, Chongqing 401331, People's Republic of China

[a)]**Author to whom correspondence should be addressed:** sfwang@cqu.edu.cn

ABSTRACT

At the atomic scale, a dislocation in a crystal possesses two equilibrium cores: One has its symmetric center at the lattice point and is referred to as the O-core; the other has its symmetric center at the middle between two neighboring lattice points and is referred to as the B-core. The possible positions (symmetric centers) of the B-core and the O-core are arrayed alternately, and the dislocation movement undergoes a sequential transformation between the two types of dislocation cores. The core with lower energy is stable, and the energy difference between the O-core and the B-core is the Peierls barrier. It is found that the stability of the core is not fixed. In some materials, the B-one core is stable, and in other materials, the O-core is stable. Furthermore, the core stability can be tuned by exerting pressure or changing the environmental temperature. Because at the stability transition point the energy difference is zero, the Peierls barrier disappears and the dislocation almost moves freely. As a consequence, material plasticity dominated by the dislocation mobility will undergo substantial change in the process of the stability transition. Therefore, it is important to understand under what condition the transition occurs. Using the variational method, the stability phase boundary in the model-parameter space is investigated and the transition condition is approximately described by an analytical equation. Furthermore, it is found that in addition to the disappearance of the Peierls barrier, the B-core and the O-core have the same width at the transition point.

I. INTRODUCTION

As a kind of structural defect of crystals, the dislocation can be theoretically viewed as a kink that is a nonlinear mode protected by the topological feature. In theory, dislocations are generally studied in the framework of the Peierls–Nabarro (P–N) model.[1,2] The classical P–N model is characterized by a nonlinear integro-differential equation that is invariant under continuous translation transformation. The dislocation represented by the kink solution of the equation can change position continuously. However, as illustrated in Fig. 1, the dislocation in equilibrium must have its position at one of the symmetric points of the lattice to make the whole core structure symmetric. A free dislocation cannot be in equilibrium if its core structure is not symmetric. There are two types of symmetric points: One is the lattice point (on site), and the other is the middle point between two neighboring lattice points. The equilibrium core with the symmetric center located at the lattice point is referred to as the O-core and the equilibrium core with the symmetric point located at the middle of two neighboring lattice points is referred to as the B-core. The O-core and the B-core generally have different energies. The core with lower energy is stable and can be observed experimentally or through molecule dynamics. For a dislocation in equilibrium, the position is given by its structural symmetry-center and the core structure varies with the types of positions. It can be observed that when the dislocation quasi-statically moves through a crystal, it alternatively transforms from one core type to the other. Dislocation movement is a sequential transformation between the O-core and the B-core. Therefore, the absolute value of the energy difference between the O-core and the B-core is the height of the Peierls barrier.

The plasticity of crystals is primarily dominated by the mobility of the dislocation. Due to the discreteness of crystal structures, a dislocation needs to overcome an energy barrier to move through a crystal. The minimum external stress that assists dislocation

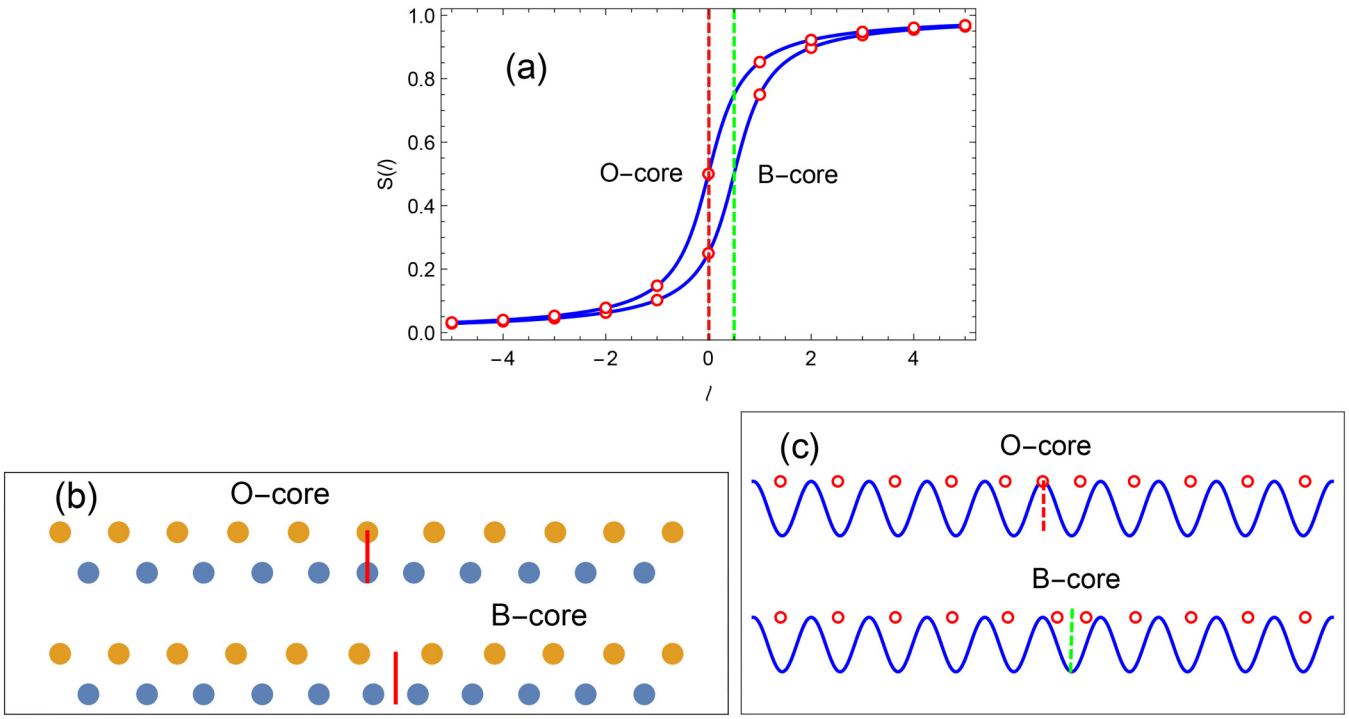

FIG. 1. (a) The two solid lines given by the kink solution Eq. (3) with the same width but different positions (symmetric centers labeled by the dashed lines) are equivalent in the continuum approximation. On atomic scale, they represent two distinct discrete core structures shown by circles. (b) Illustration of atom configurations of the O-core and the B-core. (c) If the O-core is at the top of the periodical Peierls potential, the B-core will be at the valley. The energy difference between the O-core and the B-core is the Peierls barrier.

climbing over the barrier and moving through crystal is named as Peierls stress or Peierls–Nabarro (P–N) stress. In the classical P–N model,[1] the Peierls stress is generally given by[1–10]

$$\sigma_p = \frac{Kb}{D} e^{-\frac{2\pi\zeta}{D}}, \tag{1}$$

where K is the dislocation energy factor, b is the Burgers vector, D is the step length (see Fig. 2), and ζ is the dislocation width. This formula describes the competition between the dislocation width ζ and the characteristic discreteness length D and has been widely used in theoretical and experimental studies of dislocations in materials.[4,7–10] Although the exact value of the Peierls stress may deviate from the formula prediction, it is usually believed that the fundamental qualitative feature of the Peierls stress is captured by this formula. For example, if the dislocation width increases, the Peierls stress should decrease as implied by the competition mechanism. However, it has recently been revealed that this is not always true.[11] Instead of changing monotonously, the Peierls stress varies oscillatorily. In particular, the lattice resistance nearly vanishes under a certain condition, and thus, in principle, the dislocation may almost move freely. The fundamental mechanism behind this phenomenon is the stability transition between the B-core and the O-core.[11] It is found that the core stability is not fixed. In some materials, the B-core is stable, and in other materials, the O-core is stable. Furthermore, the core stability can be tuned by exerting pressure or changing the environment temperature. If the core energy is gradually tuned so that the energy difference continuously changes across the zero point, the core stability will be exchanged between the O-core and the B-core. Because the energy difference is zero at the stability transition point, the Peierls barrier disappears and the dislocation almost moves freely. Obviously, material plasticity, dominated by the dislocation mobility, will undergo substantial change in the process of stability transition. It is important to understand the condition of the stability transition as much as possible.

In this paper, based on the spectrum model of the fully discrete dislocation theory, the core stability transition and the Peierls stress are studied using the variational method and the numerical calculations. The stability phase boundary separating the core stability zones in the parameter space is determined and approximately described by an analytical equation. The content is organized as follows. Section II focuses on the classical Peierls model in which the rigid dislocation assumption is used to calculate the Peierls stress. In Sec. III, after a brief introduction of the spectrum model, the Peierls barrier, the Peierls stress, and the core stability transition are studied comprehensively. The results from the numerical calculation and the variational evaluation are consistent with each other. The last section is a summary.

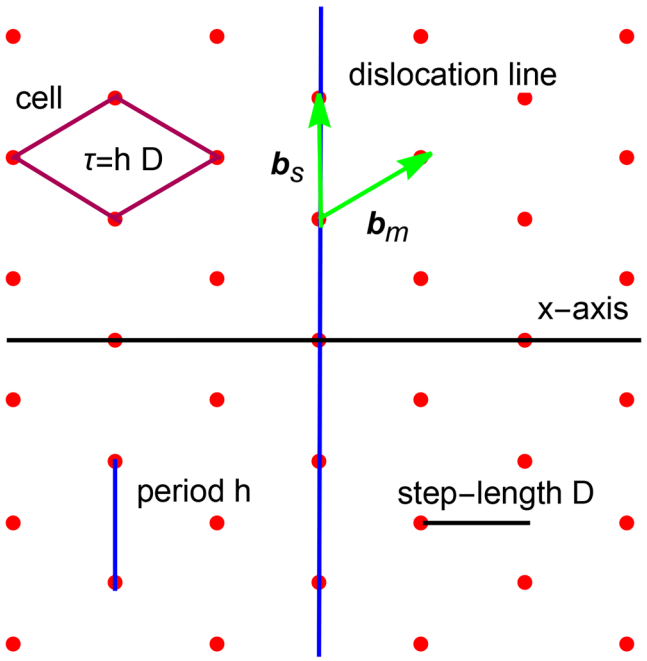

FIG. 2. A typical glide plane [(111) lattice plane in FCC crystal] and the geometrical parameters frequently involved in the dislocation theory, where $\mathbf{b}_s$ and $\mathbf{b}_m$ are, respectively, the Burgers vectors of the screw and the 60° mixed dislocations.

II. THE PEIERLS BARRIER IN THE CLASSICAL P–N MODEL

In the classical Peierls–Nabarro (P–N) model, the dislocation energy functional (energy per unit length of straight dislocation) is the sum of the elastic energy U_e and the misfit energy U_m

$$U = U_e + U_m$$

with

$$U_e = -\frac{K}{4\pi}\int_{-\infty}^{\infty}\int_{-\infty}^{\infty}\rho(x')\rho(x)\ln\frac{|x-x'|}{R}dx'dx, \quad \rho(x) = \frac{dS}{dx},$$

$$U_m = \int_{-\infty}^{\infty}\gamma(S)dx, \quad \gamma(S) = \frac{\mu_\gamma b^2}{2\pi^2 d}\sin^2\frac{\pi S}{b},$$

where $S(x)$ is the slip field (mismatch field), K is the energy coefficient factor, b is the Burgers vector, d is the spacing between the glide planes, μ_γ is the effective shear modulus defined by the plastic slip, and $R \to \infty$ is the macroscopic size of crystal. The elastic energy U_e can be obtained from the linear elasticity theory, and the dislocation energy factor K depends on the crystal structure and the dislocation feature.[12] In the isotropic approximation, the energy factor $K = \mu/(1-\nu)$ for the edge dislocation and $K = \mu$ for the screw dislocation, where μ is the shear modulus and ν is the Poisson ratio. The famous Peierls equation is[1]

$$-\frac{K}{2\pi}\int_{-\infty}^{+\infty}\frac{dx'}{x'-x}\left(\frac{dS}{dx}\right)\Big|_{x=x'} = -\frac{\mu_\gamma b}{2\pi d}\sin\left(\frac{2\pi S}{b}\right). \tag{2}$$

The equation has an exact solution[1]

$$S(x) = \frac{b}{\pi}\arctan\left(\frac{x-x_c}{\zeta_p}\right) + \frac{b}{2}, \quad \zeta_p = \frac{Kd}{2\mu_\gamma}. \tag{3}$$

This solution describes the dislocation core, which locates at the position x_c, and its shape is characterized by Peierls width ζ_p. The related density is the Lorentz-type distribution around the dislocation center x_c,

$$\rho(x) = \frac{dS}{dx} = \frac{b}{\pi}\frac{\zeta_p}{\zeta_p^2 + (x-x_c)^2}.$$

Because of the discreteness of crystal structures, the slip field is actually defined on the discrete points of the glide plane, which is a two-dimensional lattice. A typical glide plane is plotted in Fig. 2, which is the (111) lattice plane of the FCC crystal. For study of a straight dislocation, it is reasonable to view the glide plane as a family of equally spaced lines that parallel with the dislocation. Let us denote the period length along the lines by h and denote the distance between two neighboring lines by D, and thus, the area of the primitive cell of the glide plane is $\tau = Dh$ (see Fig. 2). In the classical P–N model, the continuous envelope given by the Peierls solution is assumed to be invariant as the dislocation moves. When each individual line is labeled by an integer l, the discrete slip field $S(l)$ as a function of discrete variable l is assumed to be

$$S(l) = S(x)|_{x=lD} = \frac{b}{\pi}\arctan\left(\frac{lD-x_c}{\zeta_p}\right) + \frac{b}{2}. \tag{4}$$

In the continuous approximation, the dislocation position coordinates x_c may take any value because the Peierls equation is symmetric under the continuous translation transformation. However, as long as the lattice discreteness breaks continuous translation symmetry, the center of dislocation in equilibrium can only take some discrete positions because the core structure must be symmetrical. As illustrated in Ref. 11 [or Fig. 4(c)], there are two different types of equilibrium positions: The first type is $x_c = jD$ ($j = 0, \pm1, \pm2, \ldots$), i.e., the dislocation symmetric center locates at the lattice point (dislocation line coincides with a lattice line); the second type is $x_c = (j+1/2)D$ ($j = 0, \pm1, \pm2, \ldots$), i.e., dislocation symmetric center locates at the midpoint between two neighboring lattice points. The core with the symmetric center just on the lattice point is referred to as the O-core (or O-mode), and the core with the symmetry center between two neighboring lattice points is referred to as the B-core (or B-mode). Obviously, the O-core is different from the B-core even though they have the same continuous envelope function. The dislocation core in the continuous theory splits into two distinct cores in the discrete theory. Therefore, in addition to the core

width, new index (core type) should be introduced to uniquely specify the dislocation core.

The dislocation can move through the crystal when a sufficiently strong external stress field is applied. For the slowly moving (quasi-static process), the dislocation sees a periodic world due to the periodic structure of a crystal. As a consequence, the dislocation energy changes periodically with the dislocation position,

$$U(x_c + D) = U(x_c).$$

The length D will be referred to as the step length because the dislocation repeats itself after moving a distance D. In physics, it is instructive to view energy $U(x_c)$ as a potential energy function (Peierls potential) of the dislocation. The force associated with this potential energy function is

$$F(x_c) = -\frac{dU}{dx_c}.$$

In the quasi-static approximation, the resolved external stress σ satisfies the relationship $F = \sigma b$,[12] and thus,

$$\sigma(x_c) = \frac{F(x_c)}{b} = -\frac{1}{b}\frac{dU}{dx_c}.$$

In order to obtain the potential energy function $U(x_c)$, the discrete slip field given by Eq. (4) is used for arbitrary position x_c in the classical P–N model, and the misfit energy is changed into discrete sum

$$U_m(x_c) = \sum_{l=-\infty}^{\infty} \gamma(S(l))D, \quad \gamma(S(l)) = \frac{\mu_\gamma b^2}{2\pi^2 d}\sin^2\frac{\pi S(l)}{b}.$$

As for the elastic energy, it can be proved that in the harmonic approximation of lattice dynamics the elastic energy is given by[6]

$$U_e(x_c) = -\frac{1}{2}\sum_{l=-\infty}^{\infty}\frac{\partial\gamma}{\partial S(l)}S(l)D.$$

By using the slip field $S(l)$ given by Eq. (4), the misfit energy $U_m(x_c)$ can be calculated explicitly[5] (also see Appendix A),

$$U_m(x_c) = \frac{Kb^2}{4\pi}\chi(\bar{\zeta}_p, \alpha), \quad \chi(\bar{\zeta}_p, \alpha) = \frac{\sinh(2\pi\bar{\zeta}_p)}{\cosh(2\pi\bar{\zeta}_p) - \cos(2\pi\alpha)},$$

where $\bar{\zeta}_p = \zeta_p/D$ and $\alpha = x_c/D$ are, respectively, the scaled Peierls width and the position coordinates. The elastic energy $U_e(x_c)$ can be expressed as (Appendix A)

$$U_e(x_c) = \frac{Kb^2}{4\pi}\int_1^\infty \frac{\varepsilon\chi(\varepsilon\bar{\zeta}_p, \alpha) - \chi(\bar{\zeta}_p, \alpha)}{\varepsilon^2 - 1}d\varepsilon.$$

Since the dislocation energy logarithmically diverges, it is rational to introduce energy relative to that of the O-core ($x_c = 0$),

$$E_m(x_c) = U_m(x_c) - U_m(0) = \frac{Kb^2}{2\pi}\phi(\bar{\zeta}_p, \alpha)\sin^2(\pi\alpha), \quad \phi(\bar{\zeta}_p, \alpha) = \frac{\coth\left(\pi\bar{\zeta}_p\right)}{\cos(2\pi\alpha) - \cosh(2\pi\bar{\zeta}_p)},$$

$$E_e(x_c) = U_e(x_c) - U_e(0) = \frac{Kb^2}{2\pi} \times \sin^2(\pi\alpha) \times \int_1^\infty \frac{\varepsilon\phi(\varepsilon\bar{\zeta}_p, \alpha) - \phi(\bar{\zeta}_p, \alpha)}{\varepsilon^2 - 1}d\varepsilon,$$

$$E(x_c) = E_e(x_c) + E_m(x_c) = \frac{Kb^2}{2\pi} \times \sin^2(\pi\alpha) \times \left(\int_1^\infty \frac{\varepsilon\phi(\varepsilon\bar{\zeta}_p, \alpha) - \phi(\bar{\zeta}_p, \alpha)}{\varepsilon^2 - 1}d\varepsilon + \phi(\bar{\zeta}, \alpha)\right).$$

The related stress can be expressed as

$$\sigma(x_c) = -\frac{1}{b}\frac{\partial E}{\partial x_c} = \frac{Kb}{D} \times \sin(2\pi\alpha) \times \left(\int_1^\infty \frac{\varepsilon\psi(\varepsilon\bar{\zeta}_p, \alpha) - \psi(\bar{\zeta}_p, \alpha)}{\varepsilon^2 - 1}d\varepsilon + \psi(\bar{\zeta}_p, \alpha)\right), \quad (5)$$

$$\psi(\bar{\zeta}_p, \alpha) = \frac{\sinh(2\pi\bar{\zeta}_p)}{2(\cosh(2\pi\bar{\zeta}_p) - \cos(2\pi\alpha))^2}, \quad \alpha = \frac{x_c}{D}.$$

The first term (integral term) in the parentheses results from the elastic energy, and the second term results from the misfit energy.

The difference between the B-core energy and the O-core energy is usually defined as the Peierls barrier, which can be written as

$$E_p = E(x_c)|_{x_c=\frac{D}{2}} = \frac{Kb^2}{2\pi}\left(\int_1^\infty \frac{\operatorname{csch}(2\pi\bar{\zeta}_p) - \varepsilon\operatorname{csch}(2\pi\varepsilon\bar{\zeta}_p)}{\varepsilon^2 - 1}d\varepsilon - \operatorname{csch}(2\pi\bar{\zeta}_p)\right). \quad (6)$$

In Fig. 3(a), the Peierls barrier E_p is plotted as a function of the Peierls width ζ_p. As shown in Fig. 3(a), there is a critical point $\zeta_p = 0.3923D$, at which $E_p = 0$, i.e., the B-core and the O-core have the same energy. For the wide width $\zeta_p > 0.3923D$, $E_p > 0$, energy

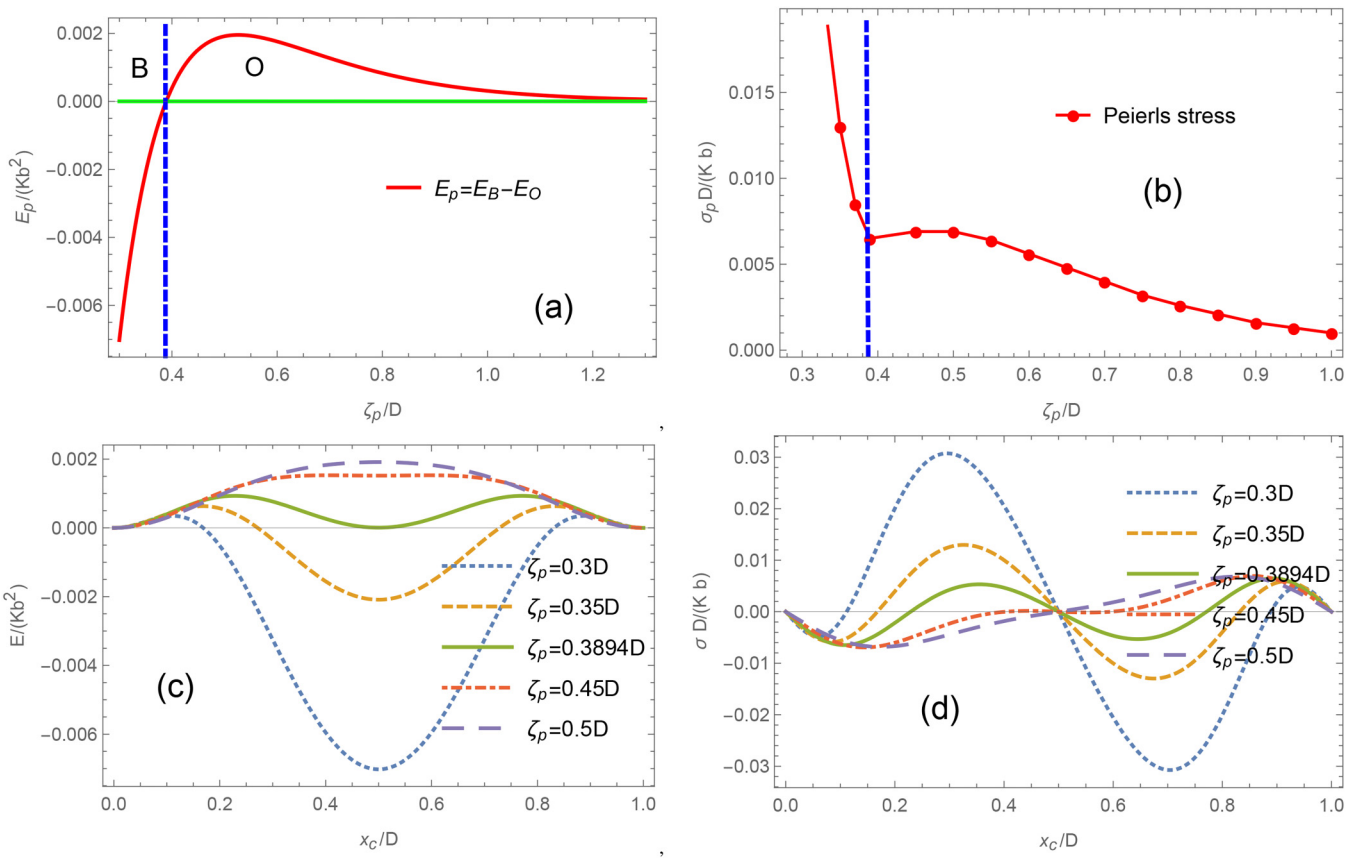

FIG. 3. (a) The Peierls barrier and the stability transition at $\zeta_p = 0.3923D$. For the narrow dislocation $\zeta_p < 0.3923D$, the B-type dislocation is stable, and for the wide dislocation $\zeta_p > 0.3923D$, the O-type dislocation is stable. (b) The relation between the Peierls stress and the Peierls width. (c) The Peierls potential as a function of the dislocation position. (d) The external stress needed to balance the force produced by the Peierls potential.

of the B-core is higher than that of the O-core. For the narrow width $\zeta_p < 0.3923D$, $E_p < 0$, energy of the B-core is lower than that of the O-core. Therefore, the O-core is stable if $\zeta_p > 0.3923D$, and the B-core is stable if $\zeta_p < 0.3923D$. In conclusion, the core stability is not fixed but dependent on the core width in the classical P–N model. In addition, from Fig. 3(c), it can be seen that for the narrow dislocation, the Peierls potential $E(x_c)$ does not monotonically vary in the range $0 < x_c < D/2$. Although the O-core is unstable in global for $\zeta_p < 0.3923D$, it is stable locally.

The maximum value of the stress $\sigma(x_c)$ is the Peierls stress,

$$\sigma_p = \max|\sigma(x_c)| = \max\left|\frac{1}{b}\frac{dE(x_c)}{dx_c}\right|.$$

As shown in Fig. 3(b), the Peierls stress falls off as the width increases. However, it does not fall off monotonously. There is a minimum at the critical point $\zeta_p = 0.3923D$. The Peierls stress is not zero at the critical point although the Peierls barrier vanishes. This conclusion is clearly confirmed by Fig. 3(d) where the stress is plotted as a function of the dislocation position coordinates. The unusual behavior of the Peierls stress originates from considering the elastic energy contribution. If the contribution from the elastic energy is cancelled, the Peierls stress varies in a simple way. In particular, the formula Eq. (1) of the Peierls stress can be readily obtained form Eq. (5) for the wide dislocation.

III. THE STABILITY TRANSITION CONDITION IN THE SPECTRUM MODEL

In the framework of Peierls theory of dislocations, the fully discrete dislocation equation can be properly obtained from the spectrum model.[11,13] In the spectrum model, as a functional of discrete slip field $S(l)$, the elastic energy U_e in a period length h of a straight dislocation is given by[13]

$$U_e = \frac{\omega^{(2)}}{8}\sum_{l=-\infty}^{\infty}\rho^2(l) - \frac{\omega^{(1)}}{4\pi}\sum_{l=-\infty}^{\infty}\sum_{l'=-\infty}^{\infty}\rho(l)\rho(l')\psi^{(0)}\left(|l-l'|+\frac{1}{2}\right) + \frac{Kb^2h}{4\pi}\ln\frac{R}{D}, \quad (7)$$

where $\rho(l) = S(l+1) - S(l)$, $\psi^{(0)}(z)$ is the polygamma function that coincides with the logarithmic function as $|z| > 1$ and has no singularity at the origin $z = 0$, and $\omega^{(1)}$ and $\omega^{(2)}$ are two physical parameters. Instead of the energy per unit length addressed frequently in the continuous theory, it is suitable to deal with the energy in a period length h of a straight dislocation in the discrete theory.

It is instructive to interpret $\rho(l)$ as local dislocation (similar to the infinitesimal dislocation proposed by Eshelby[14]) at the site l because sum of all local dislocations equals to the Burgers vector,

$$\sum_l \rho(l) = S(\infty) - S(-\infty) = b.$$

In the concept of local dislocation, a global dislocation is composed of local dislocations, and thus, a dislocation core structure is just a distribution of local dislocations. It should be noted that although $\rho(l)$ is defined similarly to the dislocation density $\rho(x)$ introduced in Sec. II, but their physical units are different. The $\rho(l) \sim \rho(x)dx$ ($dx = D$) can be roughly viewed as the lattice version of the infinitesimal dislocation proposed by Eshelby[14]). In the dislocation theory, the elastic energy U_e is physically interpreted as the total interaction energy of the local dislocations. According to the interaction theory, the first term in Eq. (7) represents the point-contact interaction, and the second term represents the long-range interaction described by the Polygamma function. The last term in Eq. (7) is just the total energy obtained in the elastic theory for a dislocation with radius D. The long-range interaction constant can be obtained by recover of the continuum theory as a continuous limit,[13]

$$\omega^{(1)} = Kh.$$

The point-contact interaction originates from lattice discreteness, and the interaction constant, $\omega^{(2)}$ can be related to the maximum of the boundary matrix $\widetilde{\Lambda}$[13]

$$\omega^{(2)} = \frac{1}{2}\widetilde{\Lambda}^{e}_{\max} - \omega^{(1)}. \tag{8}$$

In the local approximation, the misfit energy is identified with the generalized stacking fault energy,[15,16]

$$U_m = \sum_{l=-\infty}^{\infty} \gamma(S(l))\tau, \quad \gamma(S(l)) = \frac{\mu_\gamma b^2}{2\pi^2 d}\sin^2\frac{\pi S(l)}{b}\left(1 + \Delta\sin^2\frac{\pi S(l)}{b}\right),$$

where Δ is a dimensionless parameter describing the correction to the sinusoidal force law.

The dislocation equation satisfied by the discrete slip field is[11,13]

$$\Gamma\frac{\partial S(l)}{\partial t} - \frac{\omega^{(2)}}{4}[\rho(l) - \rho(l-1)] - \frac{\omega^{(1)}}{2\pi}\sum_{l'}\frac{\rho(l')}{l' - l + \frac{1}{2}} = -\frac{\partial\gamma}{\partial S(l)}\tau + \sigma\tau, \tag{9}$$

where σ is the resolved external stress, $\tau = Dh$ is the area of the primitive cell of the glide plane that is a two-dimensional lattice, and Γ is an effective damping constant. This is a time-dependent evolution equation with the dissipation term proportional to the derivative of the slip field with regard to time. When an arbitrary input function with the dislocation boundary condition is used as the initial condition, it will spontaneously relax to the stable equilibrium solution if there is no external stress applied. Therefore, the stable dislocation core as a final configuration can be easily obtained from numerical calculation. The time-dependent equation can also be used to investigate the dislocation response behavior to the external field. In practical calculation, the classical Peierls solution is employed as the initial input, after it has relaxed to the stable dislocation solution, the external stress is applied gradually to investigate how the dislocation responds.

It is convenient to introduce dimensionless slip field,

$$\frac{S(l)}{b} \to S(l), \quad \frac{\rho(l)}{b} \to \rho(l).$$

The scaled local dislocation $\rho(l)$ becomes normalized distribution,

$$\sum_l \rho(l) = 1.$$

Furthermore, it is reasonable to measure the evolution time in units of characteristic time scale $t_s = D/c$, which is the time needed for an acoustic wave to propagate a step length D at speed c. Dividing by factor $\omega^{(1)}b$ in both sides of Eq. (9), the dislocation equation in terms of the dimensionless slip field can be written as

$$\bar{\Gamma}\frac{\partial S(l)}{\partial \bar{t}} - \frac{\beta}{4}[\rho(l) - \rho(l-1)] - \frac{1}{2\pi}\sum_{l'}\frac{\rho(l')}{l' - l + \frac{1}{2}} = -\frac{1}{4\pi\bar{\zeta}_p}\left(1 + 2\Delta\sin^2(\pi S)\right)\sin(2\pi S) + \frac{\sigma D}{Kb}, \tag{10}$$

where

$$\beta = \frac{\omega^{(2)}}{\omega^{(1)}}, \quad \bar{\zeta}_p = \frac{Kd}{2\mu_\gamma D}, \quad \bar{t} = \frac{ct}{D}, \quad \bar{\Gamma} = \frac{\Gamma c}{K\tau}.$$

For the dissipation due to wave emission from the slip planes, the damping constant approximately is $\Gamma \approx K\tau/(2c)$,[17] and thus, $\bar{\Gamma} \approx 1/2$. In fact, the exact value of the effective damping constant is of no great importance for the most results involved.

The elastic energy and the misfit energy can be written as

$$\frac{U_e}{\omega^{(1)}b^2} = \frac{\beta}{8}\sum_{l=-\infty}^{\infty}\rho^2(l) - \frac{1}{4\pi}\sum_{l=-\infty}^{\infty}\sum_{l'=-\infty}^{\infty}\rho(l)\rho(l')\psi^{(0)}\left(|l - l'| + \frac{1}{2}\right) + \frac{1}{4\pi}\ln\frac{R}{D}, \tag{11}$$

$$\frac{U_m}{\omega^{(1)}b^2} = \frac{1}{4\pi^2\bar{\zeta}_p}\sum_{l=-\infty}^{\infty}\left(1 + \Delta\sin^2(\pi S)\right)\sin^2(\pi S).$$

The total energy (core energy) measured in unit of $\omega^{(1)}b^2$ is

$$U=\frac{\beta}{8}\sum_{l=-\infty}^{\infty}\rho^2(l)-\frac{1}{4\pi}\sum_{l=-\infty}^{\infty}\sum_{l'=-\infty}^{\infty}\rho(l)\rho(l')\psi^{(0)}\left(|l-l'|+\frac{1}{2}\right)+\frac{1}{4\pi^2\bar{\zeta}_p}\sum_{l=-\infty}^{\infty}\sin^2\frac{\pi S(l)}{b}\left(1+\Delta\sin^2\frac{\pi S(l)}{b}\right), \tag{12}$$

where the constant term has been dropped.

For $\beta=0$ and $\Delta=0$, the dislocation equation is the discrete version of the classical Peierls equation,

$$\frac{1}{2}\frac{\partial S(l)}{\partial t}-\frac{1}{2\pi}\sum_{l'}\frac{\rho(l')}{l'-l+\frac{1}{2}}=-\frac{1}{4\pi\bar{\zeta}_p}\sin(2\pi S)+\frac{\sigma D}{Kb}.$$

This equation has only one free parameter $\bar{\zeta}_p$ that is the ratio of the Peierls width ζ_p to the step length D. It has been solved numerically to explore the discrete slip field and relationship between the Peierls stress σ_p and the parameter $\bar{\zeta}_p$. The calculated Peierls stress as a function of parameter $\bar{\zeta}_p$ is plotted in Fig. 4(a). It is found that the Peierls stress can be well described by

$$\sigma_p=0.2\pi\times\frac{Kb}{D}e^{-\frac{2\pi\zeta_p}{D}}.$$

If the factor 0.2π is dropped, this expression is the same as Eq. (1), where contribution to the Peierls barrier from the misfit energy is considered only and the leading-term approximation is used.[5,6] In the long history of P–N model, the strain energy is assumed to be nearly invariant when dislocation moves, and so the Peierls stress is dominated by the misfit energy. It is somewhat surprising that prediction with this assumption qualitatively agrees with that given in the spectrum model. In contrast, if both the contributions from the misfit energy and the elastic energy are considered as it is done in Sec. II, the qualitative discrepancy appears for the narrow dislocation as shown in Fig. 4(a). The numerically calculated slip field and the local dislocation distribution are plotted in Figs. 4(c) and 4(d). It is found that the local dislocation can be well described by the discrete Lorentz distribution,

$$\rho_0(l)=\frac{Y(l)}{Q_0},\quad Y(l)=\frac{1}{\bar{\zeta}^2+(l-\alpha)^2},\quad \bar{\zeta}=\frac{\zeta}{D}, \tag{13}$$

where ζ is the characteristic width. α specifies dislocation position, and Q_0 is a normalization constant

$$Q_0=\frac{\pi}{\bar{\zeta}}\frac{\sinh(2\pi\bar{\zeta})}{\cosh(2\pi\bar{\zeta})-\cos(2\pi\alpha)}$$

that makes

$$\sum_{-\infty}^{+\infty}\rho_0(l)=1.$$

The corresponding slip field is

$$S_0(l)=\sum_{-\infty}^{l-1}\rho_0(l')=\frac{i}{2\bar{\zeta}Q_0}[\psi^{(0)}(-l+\alpha-i\bar{\zeta}+1)-\psi^{(0)}(-l+\alpha+i\bar{\zeta}+1)], \tag{14}$$

with the boundary conditions

$$S_0(-\infty)=0,\quad S_0(\infty)=1.$$

As shown in Fig. 4(b), the width of the B-core is always larger than that of the O-core, but the difference approaches to zero as the Peierl width ζ_p increases.

The fully discrete equation of dislocation is difficult to solve. The Ritz variation evaluation is an efficient way in approximately finding the analytical solution. In Ref. 18, a trial solution was suggested,

$$\rho(l)=\frac{1}{Q}\left((1-c)Y(l)+2c\bar{\zeta}^2Y^2(l)\right)=\frac{\hat{D}Y}{Q}, \tag{15}$$

where $Q=\hat{D}Q_0$, in which $\hat{D}$ is an operator defined by

$$\hat{D}=1-c-c\bar{\zeta}\frac{\partial}{\partial\bar{\zeta}}.$$

While the variational parameter $\bar{\zeta}$ represents the dislocation width, the variational parameter c is referred to as the core structure constant.[18] The related discrete slip field is

$$S(l)=\sum_{-\infty}^{l-1}\rho(l')=\frac{\hat{D}(Q_0S_0)}{Q},\quad S(-\infty)=0,\quad S(\infty)=1. \tag{16}$$

For α takes an integer, $\alpha=l_0$, the discrete slip field satisfies relation

$$S(l-l_0)-\frac{1}{2}=\frac{1}{2}-S(-l+l_0+1),\quad l=0,\pm1,\pm2,\ldots.$$

As illustrated in Fig. 4(c), the slip field satisfies that this relation has a symmetric center located at the middle between the points l_0 and l_0+1 and, thus, represents a B-core with the position coordinates $x_c=(l_0+1/2)D$. The possible positions of a B-core arrayed periodically with the period D. All the B-cores at different positions are actually equivalent and have the same energy,

$$U|_{\alpha=l_0}=U|_{\alpha=0}=U_B,\quad l_0=\pm1,\pm2,\ldots.$$

The core width $\bar{\zeta}$ and the core structure constant c for the B-core in equilibrium can be obtained by finding the minimum of the energy function $U_B(\bar{\zeta},c)$, and the minimum energy is just the dislocation energy in equilibrium.

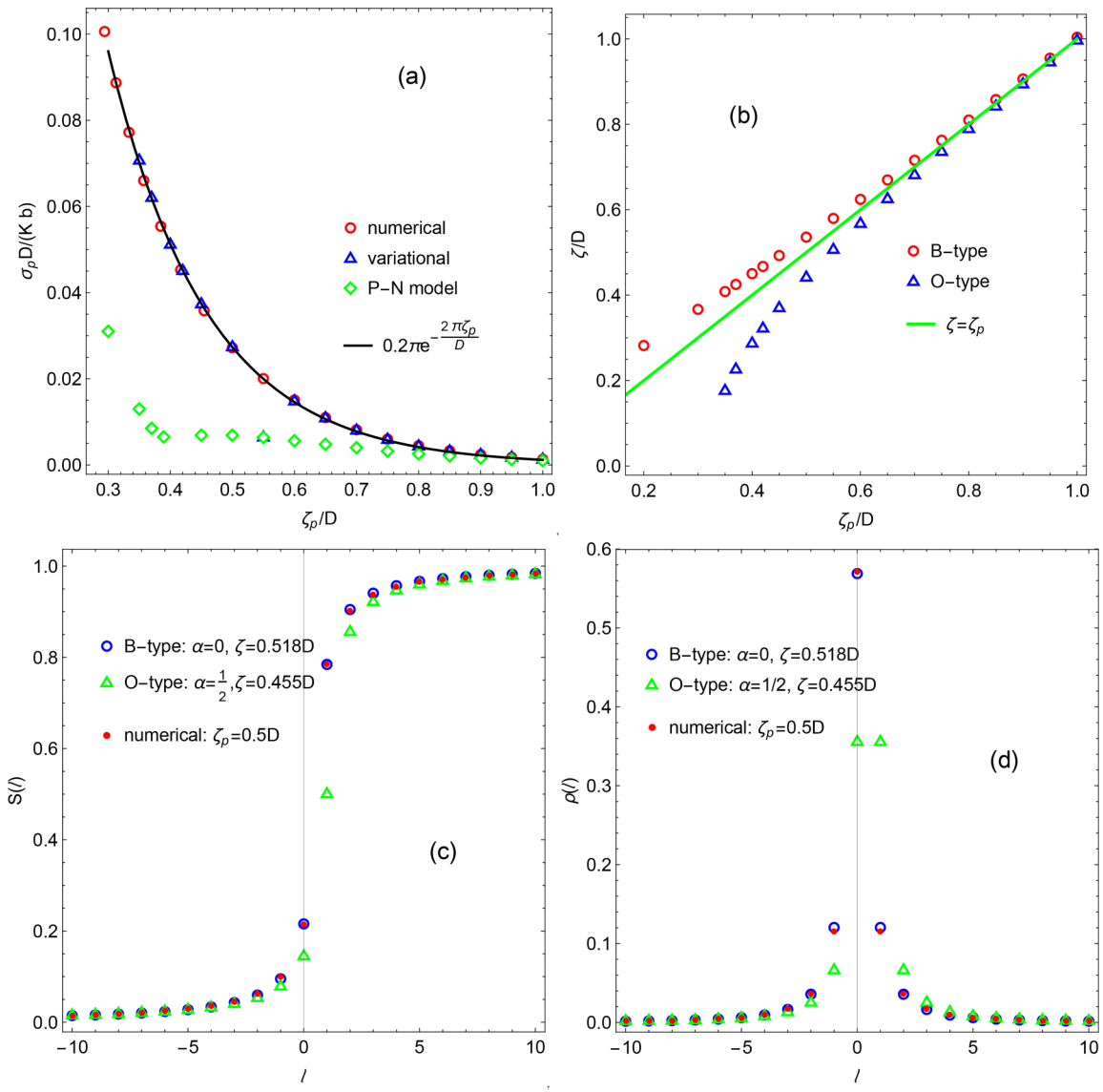

FIG. 4. (a) The Peierls stress in the case $\beta = 0$ and $\Delta = 0$. The data from the numerical calculation and the variational evaluation can be perfectly fitted by expression similar to Eq. (1). The data labelled by diamonds are from Fig. 3(b) in Sec. II. (b) The dislocation width from the variational evaluation. The O-core is always narrower than the B-core. (c) Typical slip fields. The unstable O-core automatically relaxes to the B-core in the numerical calculation. (d) Typical local dislocation distributions. The local dislocation distributions given by the numerical solution and the variational solution are satisfactorily agreement.

For α takes a half-integer, $\alpha = l_0 + 1/2$, the discrete slip field satisfies the following relation:

$$S(l - l_0) - \frac{1}{2} = \frac{1}{2} - S(-l + l_0 + 2), \quad l = 0, \pm 1, \pm 2, \ldots.$$

As illustrated in Fig. 4(c), the slip field satisfies that this relation has a symmetric center located at point $l_0 + 1$ and, thus, represents an O-core with the position coordinates $x_c = (l_0 + 1)D$. The slip at the symmetric center is always fixed to be $S = 1/2$ for the O-core.

Similar to the B-core, the possible positions of an O-core also arrayed periodically with the period D, and the energy of an O-core is given by

$$U_{\alpha=l_0+\frac{1}{2}} = U|_{\alpha=\frac{1}{2}} = U_o, \quad l_0 = \pm 1, \pm 2, \ldots,$$

and thus, the variational parameters and the dislocation energy for the O-core in equilibrium can be obtained by finding the minimum of the energy function $U_O(\bar{\zeta}, c)$.

The possible positions of the B-core and the O-core are arrayed alternately. Besides their positions, the B-core and the O-core may have different core width $\bar{\zeta}$, different structure constant c, and different energy in the discrete theory. When the O-core quasi-statically moves forward (or backward) half a step length D, it transforms into the B-core. Dislocation movement is a sequent transformation between two types of dislocation,

$$O \to B \to O \to B \to O \to B \to O \to B \cdots.$$

The Peierls barrier is defined as the energy difference between the B-core and the O-core,

$$E_p = U_B - U_O.$$

For the quasi-static movement of a dislocation, it can be further assumed that the dislocation possesses a unique structure at an arbitrary position, and the dislocation energy is a periodically continuous function of the position coordinates x_c,

$$U(x_c + D) = U(x_c).$$

Expanding $U(x_c)$ into the Fourier series and keeping the leading term only, the energy function becomes

$$U(x_c) = \frac{1}{2}(U_B + U_O) - \frac{1}{2}(U_B - U_O)\cos\frac{2\pi x_c}{D}. \tag{17}$$

In this leading term approximation, the Peierls stress is proportional to the magnitude of the Peierls barrier,

$$\sigma_p = \frac{\pi|E_p|}{bD}. \tag{18}$$

In the variation evaluation, it is suitable to introduce the overlap function,

$$L(l) = \sum_{l'=-\infty}^{\infty} \rho(l')\rho(l'-l),$$

and change the energy expression Eq. (12) into the following form:[18]

$$U = \frac{\beta}{8}L(0) + \sum_{l=-N}^{l=N}\left(-\frac{1}{4\pi}L(l)\psi^{(0)}\left(|l| + \frac{1}{2}\right) + \frac{1}{4\pi^2\bar{\zeta}_p}\sin^2\frac{\pi S(l)}{b}\left(1 + \Delta\sin^2\frac{\pi S(l)}{b}\right)\right), \quad N \to \infty. \tag{19}$$

For the trial solution given above, $L(l)$ can be calculated explicitly (see Appendix B), and the energy U can be obtained approximately with a large enough N ($N = 200$ is chosen in the practical variational evaluation). In addition, an approximated relationship can be derived for structure constant c and width $\bar{\zeta}$ from the asymptotical analysis (see Appendix C),

$$c = \frac{-2\bar{\zeta} + i\bar{\zeta}_p\cot(\pi(\alpha + i\bar{\zeta})) - i\bar{\zeta}_p\cot(\pi(\alpha - i\bar{\zeta}))}{\bar{\zeta}\left(\pi\bar{\zeta}_p\csc^2(\pi(\alpha + i\bar{\zeta})) + \pi\bar{\zeta}_p\csc^2(\pi(\alpha - i\bar{\zeta})) - 2\right)},$$

and in particular, for the B-core and the O-core,

$$c_B = c|_{\alpha=0} = \frac{\bar{\zeta} - \bar{\zeta}_p\coth(\pi\bar{\zeta})}{\pi\bar{\zeta}\bar{\zeta}_p\,\mathrm{csch}^2(\pi\bar{\zeta}) + \bar{\zeta}},$$

$$c_O = c|_{\alpha=\frac{1}{2}} = \frac{\bar{\zeta}_p\tanh(\pi\bar{\zeta}) - \bar{\zeta}}{\pi\bar{\zeta}\bar{\zeta}_p\,\mathrm{sech}^2(\pi\bar{\zeta}) - \bar{\zeta}}.$$

These expressions reduce the number of variational parameters and are used in the practical calculation.

In order to validate the trial solution, variational evaluation is first carried out for the case of $\beta = 0$ and $\Delta = 0$. The results are summarized in Fig. 4. From Fig. 4(a), one sees that the Peierls stress from the variational evaluation well agrees with that given by numerical calculation. It should be pointed out that the Peierls stress cannot be directly obtained from the variational evaluation (the output of the variational evaluation is the Peierls barrier). The variational data in Fig. 4(a) are calculated from Eq. (18) that is given under the leading term approximation. This fact implies that the Peierls potential function $U(x_c)$ has a simple behavior. Furthermore, it is found that the B-core always has lower energy comparing with the O-core, and thus, B-core is stable forever in the condition $\beta = 0$ and $\Delta = 0$. From Fig. 4(b), one sees that the characteristic width ζ of the B-core is wider than that of the O-core, but the width difference approaches zero as the Peierls width ζ_p increases. It is found that the structure constant $c \approx 0$ for both the B-core and the O-core. The fact indicates that the local dislocation $\rho(l)$ can be well described by the discrete Lorentz distribution as supposed to be. In Figs. 4(c) and 4(d), the slip field and the local dislocation distribution are explicitly plotted for $\zeta_p = 0.5D$. The result from the variational evaluation is satisfactorily in agreement with that obtained from the numerical calculation.

Peierls stress oscillation has been revealed clearly by solving dislocation numerically and explained by stability transition between the B-core and the O-core in Ref. 11. By using the variational method, the core energy and dislocation width are calculated for various model parameters ζ_p, β, and Δ to investigate the stability transition comprehensively. At first, the theoretical calculation really proves the existence of the transition point at which the Peierls barrier vanishes as shown in Fig. 5(a). Furthermore, from Fig. 5(b), it can be seen that the width of the B-core is wider than that of the O-core on the left-side of the transition point but becomes narrower on the right-side. Because dislocation width must be a continuous function, the transition point must be cross point, i.e., the B-core and the O-core have the same width at the transition point. Generally, dislocation width changes periodically as it slowly moves. In analogy to that the energy difference reaches the maximum, it is reasonable to believe that the width change also gets its maximum when a dislocation goes forward a half-period from a lattice point (B-core transforms into O-core). That is to say,

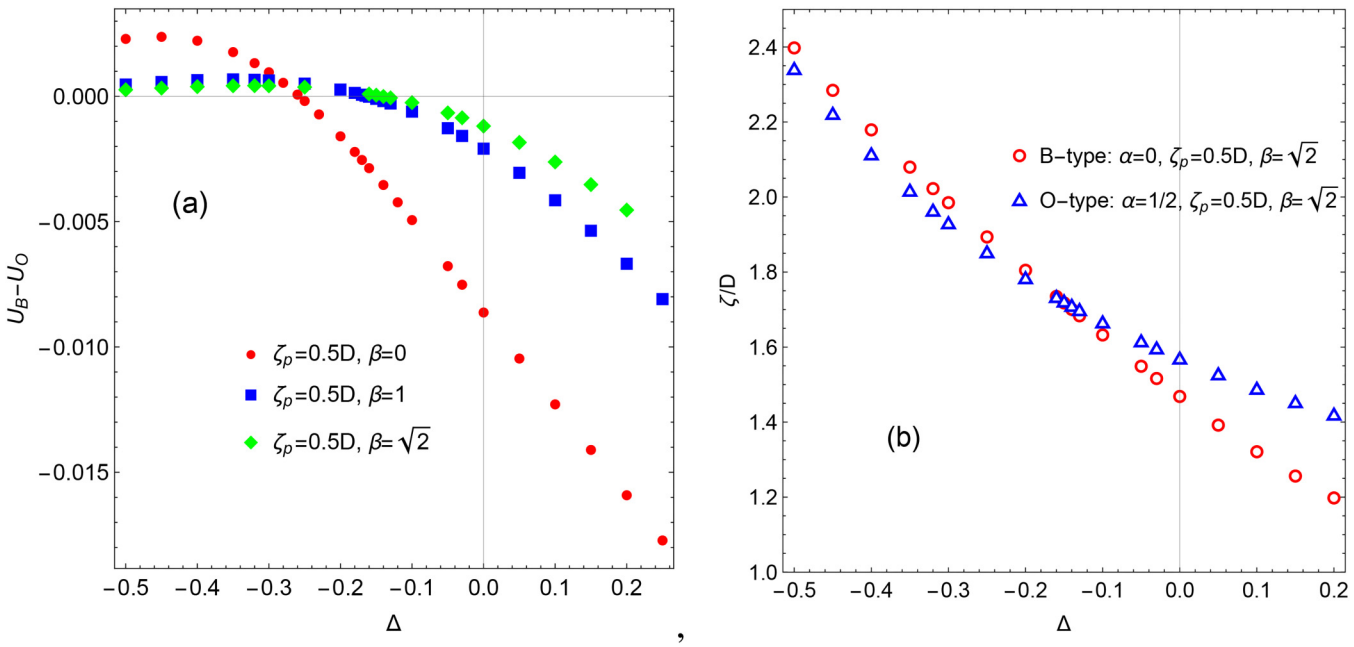

FIG. 5. (a) The Peierls barrier varies from positive value to negative value across the zero-point as the parameter Δ increases. The zero-point is the stability transition point. (b) The dislocation width decreases as the parameter Δ increases. The O-core and the B-core have the same width at the transition point.

width equality may imply that the core of a slowly moving dislocation with vanishing Peierls barrier may be invariant.

The stability transition points determined by additionally requiring $U_B = U_O$ are plotted in Fig. 6. It is found that the obtained data can be well fitted by the following equation [Fig. 6(a)]:

$$\Delta = \Delta_1(\bar{\zeta}_p, \beta) = -\frac{0.113}{\bar{\zeta}_p} e^{-\frac{\beta}{\pi}}. \tag{20}$$

This is the stability transition equation. In the parameter space, this equation determines the stability phase boundary surface [plotted in Fig. 6(c)]. For $\Delta > \Delta_1$, the B-core is stable. Across the boundary surface, the B-core lost stability, and the O-core becomes stable. However, as shown in the numerical calculation,[11] the O-core is not always stable below the surface. As parameter Δ decreases further, the O-core will lose stability and the B-core becomes stable again. There exists a series of transition surfaces, and the parameter space is separated into different stability zones by those surfaces. Unfortunately, due to limitation of the trial solution, present variation evaluation can predict the first phase boundary surface only.

It is necessary to verify the accuracy of the stability transition Eq. (20) predicted from the variational evaluation. For the pure edge dislocation in the cubic lattice, taking Poisson ratio $\nu = 1/3$, $\omega^{(2)} = 2\mu h$, $\omega^{(1)} = \mu h/(1-\nu)$, $\mu_\gamma = \mu$ (μ is the shear modulus), then

$$\beta = \frac{\omega^{(2)}}{\omega^{(1)}} = \frac{4}{3}, \quad \bar{\zeta}_p = \frac{\mu d}{2\mu_\gamma D(1-\nu)} = \frac{3}{4}.$$

Substituting into Eq. (20), the predicted value is $\Delta = -0.0985$ that coincides with the numerical result $\Delta = -0.0981$.[11] For the screw dislocation in the cubic lattice, it is suggested[13] that $\omega^{(2)} = \sqrt{2}\mu h$, $\omega^{(1)} = \mu h$, $\mu_\gamma = \mu$. The predicted value is $\Delta = -0.140$. As shown in Fig. 6(b), the value given by numerical calculation is $\Delta = -0.141$. Accuracy of the prediction from the stability transition equation exceeds expectation.

In terms of the dimensional physics parameters, the stability transition equation becomes

$$\Delta = -0.226 \times \left(\frac{\mu_\gamma D}{Kd}\right) e^{-\frac{\omega^{(2)}}{\pi K h}}. \tag{21}$$

Strictly speaking, this equation is applicable only to the pure edge dislocation or the pure screw dislocation. However, if the constrained path approximation can be used for the mixed dislocation, the two-component dislocation equation will be simplified to a single-component one that is formally identical to Eq. (9), but the parameters are given by

$$K = K_e \sin^2\theta + K_s \cos^2\theta, \quad \omega^{(2)} = \omega_e^{(2)} \sin^2\theta + \omega_s^{(2)} \cos^2\theta,$$

where K_e (K_s) is the energy factor of the edge (screw) dislocation and θ is the angle between the dislocation line and the Burgers vector. With the new interpretation, the phase boundary equation can be approximately applied to the mixed dislocation.

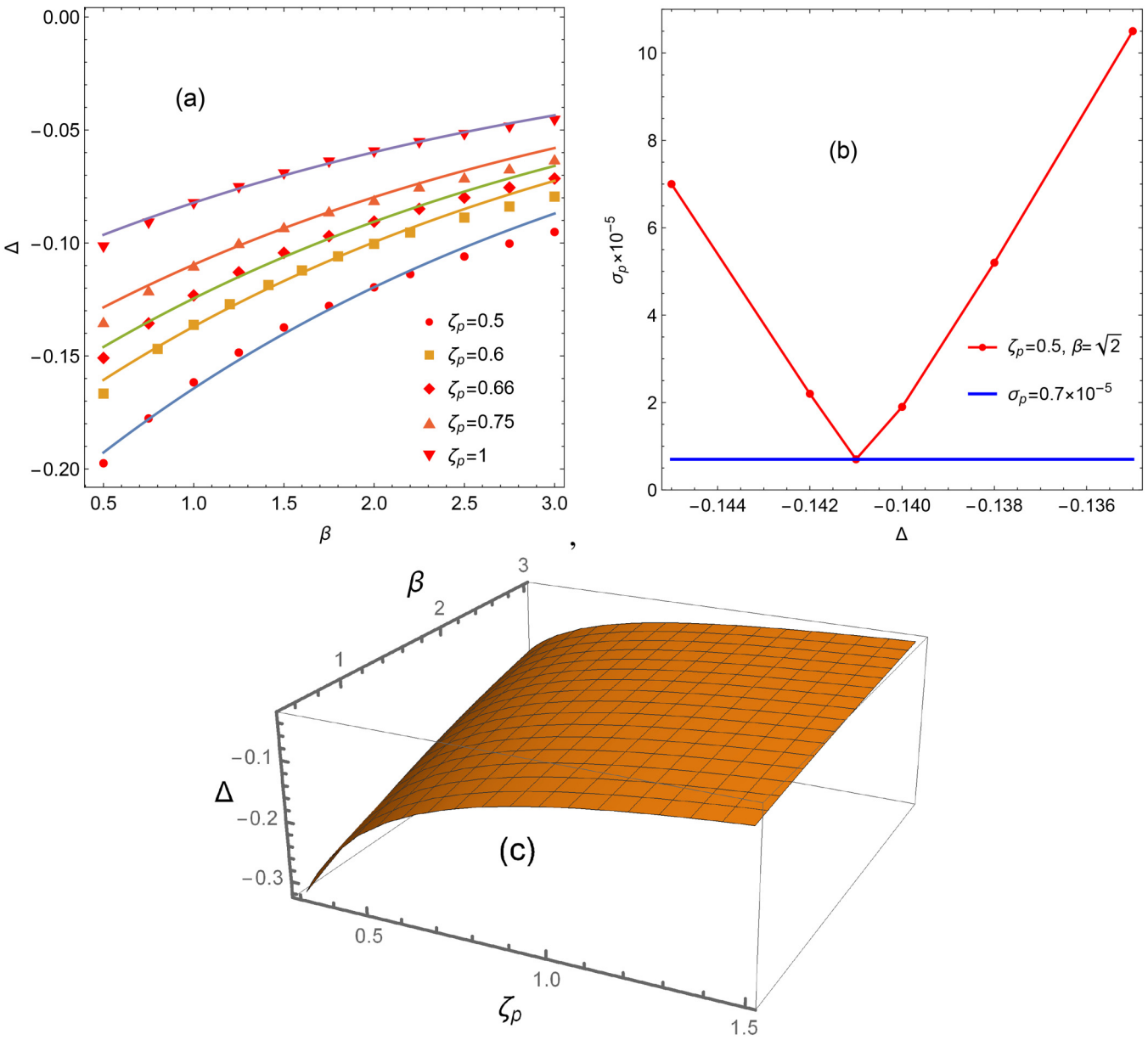

FIG. 6. (a) The scatter points are obtained from the variational evaluation under the condition $U_B = U_O$; the solid lines are given by Eq. (20) fitting from the numerical data. (b) The Peierls stress (in unit of Kb/D) is obtained from numerically solving the dislocation equation Eq. (10), and it has a local minimum of $\sigma_p \sim 0.7 \times 10^{-5} Kb/D$ at $\Delta = -0.141$. In the Δ decreasing process, the dislocation width increases, but the Peierls stress does not change monotonically as usually supposed. (c) The phase boundary surface given by Eq. (20). The B-core is stable above the surface.

IV. SUMMARY

For a dislocation, there are two types of equilibrium cores: The B-core and the O-core. The core with lower energy is stable, and the energy difference between the O-core and the B-core is the Peierls barrier. The core stability, Peierls barrier, and Peierls stress are studied for both the classical P–N model and the spectrum model. It is found that the core stability is not fixed, even in the classical P–N model, when contributions from both the misfit energy and the elastic energy are equally considered. However, such core instability does not appear in the discrete version of the classical P–N model where the rigid envelope assumption is no longer used. The present spectrum model is characterized by three

essential parameters: The first is $\bar{\zeta}_p$ (Peierls width in unit of step length D), which qualitatively measures the dislocation size; the second is β that measures the contact-interaction strength; and the third is Δ that represents correction to the sinusoidal-force law. Using variational evaluation, the stability transition equation satisfied by those parameters is obtained analytically. The results are confirmed by the numerical calculations. In the parameter space, the transition equation describes the stability phase boundary separating the core stability zone. The B-core is stable above the boundary surface and the O-core is stable below the boundary surface. Furthermore, it is found that the B-core and the O-core have the same width at the stability transition point. The stability transition may be induced by temperature (or pressure) changes.[19] The stability transition equation is helpful to look for the dislocation with vanishing Peierls barrier.

The dislocation studied in this paper is strictly limited to one that has a planar core. The concept of multiple equilibrium cores and the core stability can be generalized to the dislocation with a non-planar core, such as the screw dislocation in the BCC crystal. However, the problem is tremendously complicated for the dislocation with a non-planar core. The path of a moving dislocation with a planar core is a straight line because the dislocation has only one glide plane. In contrast, a screw dislocation in the BCC crystal has many equivalent glide planes, and the path is no longer a straight line. As a consequence, the Peierls barrier is no longer simply given by the energy difference between the O-core and B-core for the dislocation with a non-planar core. In fact, the dynamical response theory of a non-planar dislocation is still a challenge even in the framework of the P–N model.

In the P–N model, the fundamental energy function is composed of the interaction energy of the local (infinitesimal) dislocations and the misfit energy. The interaction energy is identical to the elastic energy that is obtained from the linear elastic theory for the classical P–N model or from the harmonic lattice dynamics for the spectrum model. Actually, the deformation in the dislocation core region is not small and the nonlinearity should be taken into account. In addition, the local approximation of misfit energy should also be modified to be more realistic. The effects of nonlinearity and non-locality on the stability transition condition will be investigated in the future.

ACKNOWLEDGMENTS

The author thanks Dr. Yuehui Wang for helpful suggestions and improvement in English. This work was supported by the National Natural Science Foundation of China (NNSFC) (Grant No. 12374026).

AUTHOR DECLARATIONS

Conflict of Interest

The author has no conflicts to disclose.

Author Contributions

Shaofeng Wang: Conceptualization (lead); Data curation (lead); Formal analysis (lead); Funding acquisition (lead); Investigation (lead); Methodology (lead); Project administration (lead); Resources (lead); Software (lead); Supervision (lead); Validation (lead); Visualization (lead); Writing – original draft (lead); Writing – review & editing (lead).

DATA AVAILABILITY

The data that support the findings of this study are available from the corresponding author upon reasonable request.

APPENDIX A: CALCULATION OF THE MISFIT ENERGY AND THE ELASTIC ENERGY

The detail of calculations in the Sec. II is presented here.

1. Misfit energy

The discrete slip is

$$S(l) = \frac{b}{\pi}\arctan\left(\frac{lD - x_c}{\zeta_p}\right) + \frac{b}{2} = \frac{b}{\pi}\arctan q + \frac{b}{2},$$

where

$$q = \frac{lD - x_c}{\zeta_p} = \frac{l - \alpha}{\bar{\zeta}_p}, \quad \bar{\zeta}_p = \frac{\zeta_p}{D} = \frac{Kd}{2\mu_\gamma D}, \quad \alpha = \frac{x_c}{D}.$$

From triangular identities, one has

$$\cot\left(\frac{\pi S}{b}\right) = -q, \quad \sin^2\frac{\pi S}{b} = \frac{1}{1 + \cot^2\frac{\pi S}{b}} = \frac{1}{1 + q^2},$$

$$\gamma(S) = \frac{\mu_\gamma b^2}{2\pi^2 d}\sin^2\frac{\pi S}{b} = \frac{\mu_\gamma b^2}{2\pi^2 d}\frac{1}{1 + q^2} = \frac{\mu_\gamma b^2}{2\pi^2 d}\frac{\bar{\zeta}_p^2}{\bar{\zeta}_p^2 + (l - \alpha)^2}.$$

By using the sum formula (Appendix B),

$$\sum_{l=-\infty}^{\infty}\frac{1}{\bar{\zeta}_p^2 + (l - \alpha)^2} = \frac{\pi}{\bar{\zeta}_p}\frac{\sinh(2\pi\bar{\zeta}_p)}{\cosh(2\pi\bar{\zeta}_p) - \cos(2\pi\alpha)},$$

one has

$$U_m = \sum_{l=-\infty}^{\infty}\gamma(S(l))D = \frac{\mu_\gamma b^2 D}{2\pi^2 d}\sum_{l=-\infty}^{\infty}\frac{\bar{\zeta}_p^2}{\bar{\zeta}_p^2 + (l - \alpha)^2} = \frac{Kb^2}{4\pi}\chi(\bar{\zeta}_p, t),$$

$$\chi(\bar{\zeta}_p, t) = \frac{\sinh(2\pi\bar{\zeta}_p)}{\cosh(2\pi\bar{\zeta}_p) - \cos(2\pi\alpha)}.$$

2. Elastic energy

Because

$$\sin\frac{2\pi S}{b} = \frac{2\cot\frac{\pi S}{b}}{1 + \cot^2\frac{\pi S}{b}} = -\frac{2q}{1 + q^2},$$

one has

$$-\frac{\partial\gamma}{\partial S(l)} = -\frac{\mu_\gamma b}{2\pi d}\sin\left(\frac{2\pi S}{b}\right) = \frac{\mu_\gamma b}{2\pi d}\frac{2q}{1+q^2}.$$

The elastic energy

$$\begin{aligned} U_e &= -\frac{1}{2}\sum_{l=-\infty}^{\infty}\frac{\partial\gamma}{\partial S(l)}S(l)D = -\frac{1}{2}\sum_{l=-\infty}^{\infty}\frac{\mu_\gamma bD}{2\pi d}\sin\left(\frac{2\pi S}{b}\right)S(l) \\ &= \frac{\mu_\gamma bD}{4\pi d}\sum_{l=-\infty}^{\infty}\frac{2q}{1+q^2}\times\left(\frac{b}{\pi}\arctan q+\frac{b}{2}\right) \\ &= \frac{\mu_\gamma b^2 D}{2\pi^2 d}\sum_{l=-\infty}^{\infty}\frac{q\arctan q}{1+q^2}\Big|_{q=(l-\alpha)/\bar{\zeta}_p}, \end{aligned}$$

where the constant slip $b/2$ has been canceled in the last equality because a global translation has no contribution. The sum in the equation can be changed into an integration. Introducing a parameterized sum,

$$M(\varepsilon) = \sum_{l=-\infty}^{\infty}\frac{q\arctan(\varepsilon q)}{1+q^2},$$

obviously

$$U_e = \frac{\mu_\gamma b^2 D}{2\pi^2 d}M(1), \quad M(0) = 0.$$

Taking differential with regard to parameter ε

$$\begin{aligned} \frac{\partial M}{\partial\varepsilon} &= \sum_{l=-\infty}^{\infty}\frac{q^2}{(1+q^2)(1+\varepsilon^2q^2)} \\ &= \frac{1}{1-\varepsilon^2}\sum_{l=-\infty}^{\infty}\left(\frac{1}{1+\varepsilon^2q^2}-\frac{1}{1+q^2}\right)\Big|_{q=(l-\alpha)/\bar{\zeta}_p}, \end{aligned}$$

the right-hand side can be calculated explicitly

$$\frac{\partial M}{\partial\varepsilon} = \frac{1}{1-\varepsilon^2}\left(\frac{\pi\bar{\eta}_p\sinh(2\pi\bar{\eta}_p)}{\cosh(2\pi\bar{\eta}_p)-\cos(2\pi\alpha)}-\frac{\pi\bar{\zeta}_p\sinh(2\pi\bar{\zeta}_p)}{\cosh(2\pi\bar{\zeta}_p)-\cos(2\pi\alpha)}\right),$$

$$\bar{\eta} = \frac{\bar{\zeta}_p}{\varepsilon},$$

and thus,

$$M(1) = \int_0^1\frac{\partial M}{\partial\varepsilon}d\varepsilon = \int_0^1\frac{\pi\bar{\eta}_p\chi(\bar{\eta}_p,\alpha)-\pi\bar{\zeta}_p\chi(\bar{\zeta}_p,\alpha)}{1-\varepsilon^2}d\varepsilon.$$

Substituting into the elastic energy expression, one obtains the expression in the text,

$$\begin{aligned} U_e &= \frac{Kb^2}{4\pi}\int_0^1\frac{d\varepsilon}{1-\varepsilon^2}\left(\frac{1}{\varepsilon}\chi\left(\frac{\bar{\zeta}_p}{\varepsilon},\alpha\right)-\chi(\bar{\zeta}_p,\alpha)\right) \\ &= \frac{Kb^2}{4\pi}\int_1^\infty\frac{\varepsilon\chi(\varepsilon\bar{\zeta}_p,\alpha)-\chi(\bar{\zeta}_p,\alpha)}{\varepsilon^2-1}d\varepsilon, \end{aligned}$$

in the last step, integration variable change $\varepsilon \to 1/\varepsilon$ is taken.

APPENDIX B: CALCULATION OF SUMMATION

All summations in text can be carried out based on the following formula:

$$\sum_{l=-\infty}^{\infty}\frac{1}{l+z} = \pi\cot(\pi z).$$

For example,

$$Y(l,x) = \frac{1}{x^2+(l-\alpha)^2} = \frac{i}{2x}\left(\frac{1}{l-\alpha+ix}-\frac{1}{l-\alpha-ix}\right),$$

$$\begin{aligned} Q_0 &= \sum_{l=-\infty}^{\infty}Y(l,x) = \frac{\pi}{2x}(\coth(\pi x+i\pi\alpha)+\coth(\pi x-i\pi\alpha)) \\ &= \frac{\pi}{x}\frac{\sinh(2\pi x)}{\cosh(2\pi x)-\cos(2\pi\alpha)}, \end{aligned}$$

and

$$\begin{aligned} P(x,y,j) &= \sum_{l=-\infty}^{\infty}Y(l,x)Y(l-j,y) \\ &= \frac{\pi}{2xy}\left(\frac{y\coth(\pi(x+i\alpha))}{y^2+(j+ix)^2}+\frac{y\coth(\pi(x-i\alpha))}{y^2+(j-ix)^2}\right. \\ &\quad \left.+\frac{ix\cot(\pi(\alpha+j+iy))}{x^2+(j+iy)^2}-\frac{ix\cot(\pi(\alpha+j-iy))}{x^2+(j-iy)^2}\right). \end{aligned}$$

By using the identity,

$$Y^2(l,x) = -\frac{1}{2x}\frac{\partial Y}{\partial x},$$

one has

$$\sum_{l=-\infty}^{\infty}Y^2(l,x)Y(l-j,y) = -\frac{1}{2x}\frac{\partial P}{\partial x},$$

$$\sum_{l=-\infty}^{\infty}Y(l,x)Y^2(l-j,y) = -\frac{1}{2y}\frac{\partial P}{\partial y},$$

$$\sum_{l=-\infty}^{\infty}Y^2(l,x)Y^2(l-j,y) = \frac{1}{4xy}\frac{\partial^2 P}{\partial x\partial y}.$$

Introducing

$$\rho(l,x) = a_1Y(l,x)+a_2Y^2(l,x), \quad a_1 = \frac{1-c}{Q}, \quad a_2 = \frac{2c\bar{\zeta}^2}{Q},$$

it is straightforward to obtain

$$\begin{aligned} \rho(l,x)\rho(l-j,y) &= a_1^2Y(l,x)Y(l-j,y)+a_1a_2Y^2(l,x)Y(l-j,y) \\ &\quad +a_1a_2Y(l,x)Y^2(l-j,y)+a_2^2Y^2(l,x)Y^2(l-j,y), \end{aligned}$$

$$L(x, y, j) = \sum_{l=-\infty}^{\infty} \rho(l, x)\rho(l-j, y)$$
$$= a_1^2 P - a_1 a_2 \left(\frac{1}{2x}\frac{\partial P}{\partial x} + \frac{1}{2y}\frac{\partial P}{\partial y}\right) + \frac{a_2^2}{4xy}\frac{\partial^2 P}{\partial x \partial y}.$$

The overlap function is given by

$$L(j) = L(x, y, j)|_{(x=\bar{\zeta}, y=\bar{\zeta})}.$$

The normalization factor Q can be calculated straightforwardly from Q_0,

$$Q = \hat{D}Q_0$$
$$= \frac{\pi}{2\bar{\zeta}} \times \frac{-4\pi c\bar{\zeta} + 2\cos(2\pi\alpha)(2\pi c\bar{\zeta}\cosh(2\pi\bar{\zeta}) - \sinh(2\pi\bar{\zeta})) + \sinh(4\pi\bar{\zeta})}{(\cos(2\pi\alpha) - \cosh(2\pi\bar{\zeta}))^2}.$$

APPENDIX C: ASYMPTOTICAL ANALYSIS

For $l \to -\infty$, the slip field approaches zero inversely proportional to l,

$$S(l) \to -\frac{1-c}{Q} \times \frac{1}{l},$$

and thus, the right-hand side of the dislocation equation asymptotically becomes

$$-\frac{1}{4\pi\bar{\zeta}_p}\left(1 + 2\Delta\sin^2(\pi S)\right)\sin(2\pi S) \approx -\frac{1}{2\bar{\zeta}_p} S$$
$$\approx -\frac{1}{2\bar{\zeta}_p} \times \left(-\frac{1-c}{Q} \times \frac{1}{l}\right) = \frac{1-c}{2\bar{\zeta}_p Q} \times \frac{1}{l}.$$

The left-hand side of the dislocation equation asymptotically becomes (the first term is proportional to $1/l^2$)

$$-\frac{1}{2\pi}\sum_{l'}\frac{\rho(l')}{l' - l + \frac{1}{2}}|_{l\to-\infty} \approx -\frac{\pi c\bar{\zeta}\left(\csc^2(\pi(\alpha + i\bar{\zeta})) + \csc^2(\pi(\alpha - i\bar{\zeta}))\right) - i\cot(\pi(\alpha + i\bar{\zeta})) + i\cot(\pi(\alpha - i\bar{\zeta}))}{4\bar{\zeta}Q} \times \frac{1}{l}.$$

Comparing the coefficients before $1/l$, one obtains relationship

$$c = \frac{i\bar{\zeta}_p\cot(\pi(\alpha + i\bar{\zeta})) - i\bar{\zeta}_p\cot(\pi(\alpha - i\bar{\zeta})) - 2\bar{\zeta}}{\bar{\zeta}\left(\pi\bar{\zeta}_p\csc^2(\pi(\alpha + i\bar{\zeta})) + \pi\bar{\zeta}_p\csc^2(\pi(\alpha - i\bar{\zeta})) - 2\right)}.$$

This equation can be also obtained for the case $l \to \infty$. For large $\bar{\zeta}$, the relationship is simplified into

$$c = 1 - \frac{\bar{\zeta}_p}{\bar{\zeta}} = 1 - \frac{\zeta_p}{\zeta}.$$

REFERENCES

[1]R. Peierls, "The size of a dislocation," Proc. Phys. Soc. **52**(1), 34–37 (1940).
[2]F. R. N. Nabarro, "Dislocations in a simple cubic lattice," Proc. Phys. Soc. London **59**(332), 256–272 (1947).
[3]J. N. Wang, "A new modification of the formulation of Peierls stress," Acta Mater. **44**(4), 1541–1546 (1996).
[4]J. N. Wang, "Prediction of Peierls stresses for different crystals," Mater. Sci. Eng. A **206**(2), 259–269 (1996).
[5]B. Joós and M. S. Duesbery, "The Peierls stress of dislocations: An analytic formula," Phys. Rev. Lett. **78**(2), 266–269 (1997).
[6]S. Wang, "Dislocation energy and Peierls stress: A rigorous calculation from the lattice theory," Chin. Phys. **15**(6), 1301–1309 (2006).
[7]T. Suzuki and S. Takeuchi, "Corraltion of Peierls–Nabarro stress with crystal-structure," Rev. Phys. Appl. **23**(4), 685 (1988).
[8]Y. Kamimura, K. Edagawa, and S. Takeuchi, "Experimental evaluation of the Peierls stresses in a variety of crystals and their relation to the crystal structure," Acta Mater. **61**(1), 294–309 (2013).
[9]Y. Kamimura, K. Edagawa, A. M. Iskandarov, M. Osawa, Y. Umeno, and S. Takeuchi, "Peierls stresses estimated via the Peierls–Nabarro model using ab-initio γ-surface and their comparison with experiments," Acta Mater. **148**, 355–362 (2018).
[10]K. Edagawa, Y. Kamimura, A. M. Iskandarov, Y. Umeno, and S. Takeuchi, "Peierls stresses estimated by a discretized Peierls–Nabarro model for a variety of crystals," Materialia **5**, 100218 (2019).
[11]S. Wang, "Intrinsic freedom of dislocation structures and Peierls stress oscillation," Phys. Rev. B **105**(9), 094113 (2022).
[12]J. P. Hirth and J. Lothe, "*Theory of Dislocations*, 2nd ed. (Wiley, New York, 1982).
[13]S. Zhang and S. Wang, "Global spectrum model of discrete dislocation equation," J. Appl. Phys. **136**(12), 125105 (2024).
[14]J. D. Eshelby, "The equation of motion of a dislocation," Phys. Rev. **90**(2), 248–255 (1953).
[15]J. W. Chritia and V. Vitek, "Dislocations and stacking faults," Rep. Prog. Phys. **33**(4), 3071970).
[16]S. Wang, X. Wu, and Y. Wang, "Variational principle for the dislocation equation in lattice theory," Phys. Scr. **76**(5), 593–596 (2007).
[17]Y.-P. Pellegrini, "Dynamic Peierls–Nabarro equations for elastically isotropic crystals," Phys. Rev. B **81**(2), 024101 (2010).
[18]S. Wang, S. Zhang, J. Bai, and Y. Yao, "Shape change and Peierls barrier of dislocation," J. Appl. Phys. **118**(24), 244903 (2015).
[19]H. Xiang, R. Wang, and S. Wang, "Core structure and thermal transformation of the 1/2 ⟨110⟩{111} screw dislocation in aluminum," J. Appl. Phys. **127**(12), 125106 (2020).